nature immunology

Instability of the transcription factor Foxp3 leads to the generation of pathogenic memory T cells *in vivo*

Xuyu Zhou[1,4], Samantha L Bailey-Bucktrout[1,4], Lukas T Jeker[1,4], Cristina Penaranda[1], Marc Martínez-Llordella[3], Meredith Ashby[1], Maki Nakayama[2], Wendy Rosenthal[1] & Jeffrey A Bluestone[1]

Regulatory T cells (T_{reg} cells) are central to the maintenance of immune homeostasis. However, little is known about the stability of T_{reg} cells *in vivo*. In this study, we demonstrate that a substantial percentage of cells had transient or unstable expression of the transcription factor Foxp3. These 'exFoxp3' T cells had an activated-memory T cell phenotype and produced inflammatory cytokines. Moreover, exFoxp3 cell numbers were higher in inflamed tissues in autoimmune conditions. Adoptive transfer of autoreactive exFoxp3 cells led to the rapid onset of diabetes. Finally, analysis of the T cell receptor repertoire suggested that exFoxp3 cells developed from both natural and adaptive T_{reg} cells. Thus, the generation of potentially autoreactive effector T cells as a consequence of Foxp3 instability has important implications for understanding autoimmune disease pathogenesis.

Autoimmunity represents a collection of over 80 heterogeneous disorders often controlled by complex genetic and environmental factors. The pathogenesis is thought to result from a breakdown in the mechanisms that control central and/or peripheral tolerance, which ultimately culminates in autoimmune disease. Thus, the path to effective therapies requires an understanding of the mechanisms that underlie the breakdown of tolerance normally maintained by regulatory T cells (T_{reg} cells). T_{reg} cells are a specialized $CD4^+$ T cell lineage that is central to the preservation of self-tolerance and whose dysfunction has been linked to autoimmune diseases, including type 1 diabetes[1–3]. These cells are characterized as a small subset of $CD4^+$ T cells with a unique phenotypic 'fingerprint' driven by expression of the transcription factor Foxp3 (A002750)[4]. Foxp3 is essential for the suppressive activity of T_{reg} cells, and Foxp3 deficiency leads to multiorgan autoimmune disease, as is found in scurfy mice and in human patients with immune dysregulation, polyendocrinopathy, enteropathy, X–linked syndrome[5–7]. Moreover, ectopic Foxp3 expression in non–T_{reg} cells confers suppressor function *in vitro* and *in vivo*[4]. Finally, there are two distinct subsets of T_{reg} cells in peripheral lymphoid organs: natural T_{reg} cells (nT_{reg} cells) that develop in the thymus after recognition of high-affinity self antigen, and adaptive T_{reg} cells (aT_{reg} cells) that develop from conventional T cells (T_{conv} cells) as a consequence of peripheral exposure to antigen[8]. The aT_{reg} cells serve a complementary function in maintaining peripheral tolerance, particularly for self antigens not expressed in the thymus.

Although the importance of T_{reg} cells in the control of autoimmunity is now well established, little is known about the stability of T_{reg} cells *in vivo*. Most T_{reg} cells retain high Foxp3 expression after adoptive transfer in a nonpathogenic setting, and it has been suggested that Foxp3 expression is controlled by Foxp3 itself through a positive feedback loop[9,10]. However, several studies have suggested that T_{reg} cells isolated from inflammatory sites have lower expression of Foxp3, which possibly increases susceptibility to autoimmunity[1,3]. In support of that idea, the inflammatory cytokine interleukin 6 (IL-6) acts in synergy with IL-1 to downregulate Foxp3 expression via a pathway dependent on the transcription factor STAT3 (ref. 11), and microRNA-deficient T_{reg} cells can lose Foxp3 expression[12]. In addition, peripheral T_{reg} cells, particularly the $CD4^+CD25^-Foxp3^+$ subset, are unstable in a lymphopenic setting, and those unstable T_{reg} cells can convert to follicular helper T cells and promote the formation of germinal centers in mouse Peyer's patches[13,14]. Together these findings suggest that peripheral T_{reg} cells can become unstable in certain experimental conditions.

In this study, we examine the stability of T_{reg} cells by genetic lineage tracing of $Foxp3^+$ T_{reg} cells in both homeostatic and autoimmune conditions in unmanipulated mice. We crossed transgenic mice expressing a green fluorescent protein–Cre recombinase fusion protein (GFP-Cre) controlled by the *Foxp3* promoter on a bacterial artificial chromosome (BAC; Foxp3-GFP-Cre mice)[12] with reporter mice that express yellow fluorescent protein (YFP) from the *Rosa26* promoter only after excision of a *lox*P-flanked stop cassette (Rosa26-loxP-Stop-loxP-YFP (R26-YFP) mice)[15], which allowed us to track the induction and downregulation of Foxp3 concurrently. We found that a substantial percentage of cells that at some point expressed Foxp3 had downregulated or completely lost Foxp3 expression in healthy mice; these 'exFoxp3' cells had an activated-memory phenotype and produced inflammatory cytokines. Of note, these exFoxp3 cells, which were significantly higher in percentage in the autoimmune diabetes

[1]Diabetes Center and the Department of Medicine, University of California, San Francisco, California, USA. [2]Barbara Davis Center for Childhood Diabetes, University of Colorado Denver, Aurora, Colorado, USA. [3]Present address: Liver Transplant Unit, Hospital Clínic Barcelona–August Pi Sunyer Institute for Biomedical Investigations, Barcelona, Spain. [4]These authors contributed equally to this work. Correspondence should be addressed to J.A.B. (jbluest@diabetes.ucsf.edu).

Received 18 May; accepted 18 June; published online 26 July 2009; doi:10.1038/ni.1774

setting, were able to transfer diabetes. Finally, analysis of the T cell antigen receptor-α (TCRα) variable segment (V_α) showed that the exFoxp3 cells shared ontogeny with Foxp3$^+$ T_{reg} cells as well as T_{conv} cells, which suggests that in some conditions, both nT_{reg} cells and aT_{reg} cells become unstable in the periphery and may promote autoimmunity.

RESULTS

Foxp3$^+$ T cells in Foxp3-GFP-Cre × R26-YFP mice

The Foxp3-GFP-Cre mice have been reported before[12]. Characterization of these mice has shown they have a T_{reg} cell developmental profile similar to that reported before for a Foxp3-GFP 'knock-in' reporter strain[16]. Notably, endogenous Foxp3 expression was unchanged in BAC-transgenic cells (data not shown). We crossed those mice with the R26-YFP reporter mouse[15]. In the resultant Foxp3-GFP-Cre × R26-YFP mice, Foxp3-GFP-Cre$^+$ T_{reg} cells excise the *lox*P-flanked stop cassette to drive constitutive transcription of the gene encoding YFP from the R26 promoter, which permanently marks the Foxp3$^+$ T cells and their progeny. We noted a few GFP$^+$YFP$^+$ thymocytes among CD4$^+$CD8$^+$ double-positive and CD8$^+$ single-positive (SP) thymocytes (**Fig. 1a**), which suggested that Foxp3 transcription was induced in certain conditions of exposure to self antigen during positive selection and CD8$^+$ T cell maturation. Most of the Foxp3$^+$ GFP$^+$ and/or YFP$^+$ cells were in the CD4$^+$ SP thymocyte subset (**Fig. 1a**). Using expression of heat-shock antigen (CD24) as an indicator of thymocyte maturity, we were able to map the development of the lineage (**Fig. 1b**). We found few if any GFP$^+$YFP$^+$ cells among the immature, CD4$^+$ SP, CD24^{bright} thymocytes. However, as the cells matured (indicated by lower CD24 expression), a population of GFP$^+$ cells became evident (**Fig. 1a**). These cells had low YFP fluorescence due to a delay between Foxp3 transcription, 'read out' as GFP expression, and excision of *lox*P-Stop-*lox*P in the R26-YFP transgene. Thus, the GFP$^+$YFP$^{lo–neg}$ population represented cells that had upregulated Foxp3 most recently. YFP$^+$ cells emerged as T_{reg} cells that matured further, as indicated by even lower CD24 expression, such that the most mature cells had high expression of both GFP and YFP. Thus, lineage tracing of Foxp3 promoter activity suggested that most Foxp3 transcription is initiated after the maturation of CD4$^+$ SP thymocytes. This stage of thymocyte maturation has been linked to negative selection, which supports previous suggestions that Foxp3$^+$ T_{reg} cells develop as an 'escape' mechanism during negative selection after exposure to self antigen[17,18]. Finally, the CD4$^+$ SP cells included a small but detectable cell population of GFP$^-$YFP$^+$ cells (**Fig. 1a**). This population, which constituted about 10% of the YFP$^+$ cells in the thymus, seemed to develop among the mature CD4$^+$ T cells, as all the cells were CD24^{lo}, which was consistent with their having derived from TCR-triggered antigen recognition. Notably, we did not find any YFP expression among B cells or other non–T cells in these mice, consistent with a high fidelity of Cre activity in this BAC transgene and lack of stochastic expression of YFP in other tissues.

Next we assessed the presence of various subsets in the periphery. As described before[12], the GFP-Cre construct in the BAC-transgenic mice was highly efficient. About 10% of peripheral CD4$^+$ T cells were GFP$^+$YFP$^+$, whereas we found very few (0.4%) GFP$^+$YFP^{lo} T cells

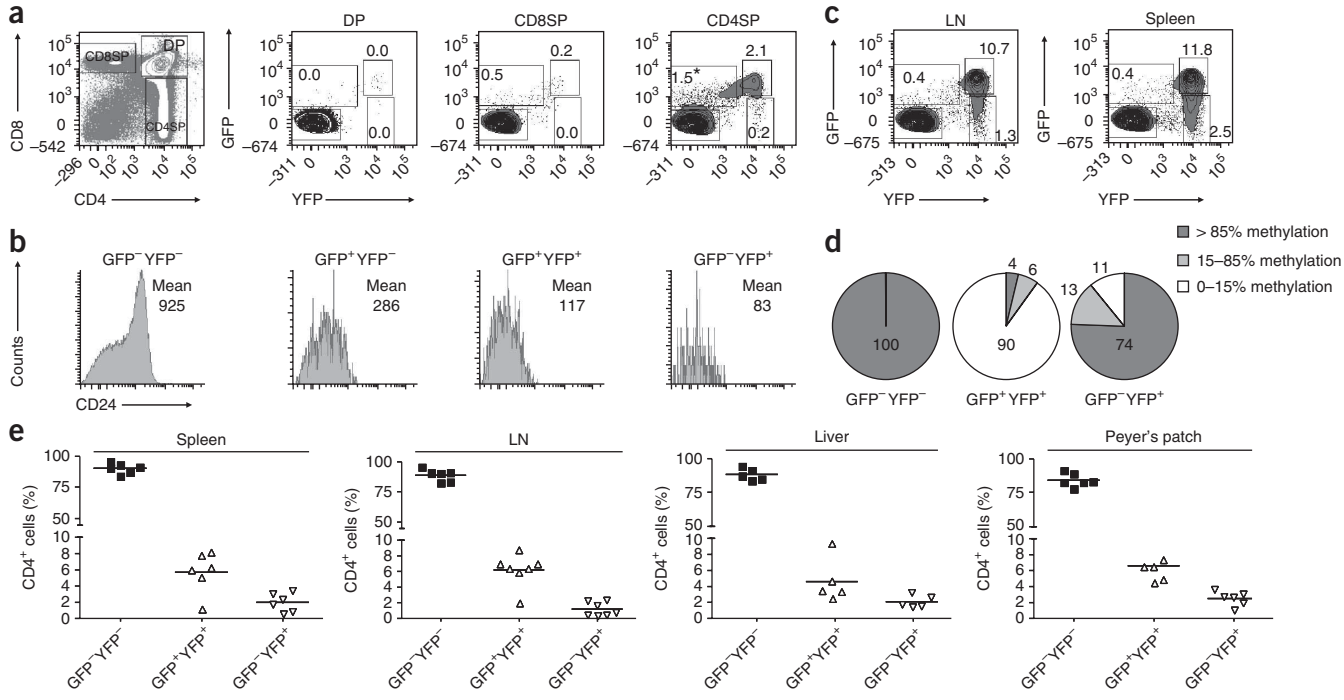

Figure 1 Development of Foxp3$^+$ T cells in Foxp3-GFP-Cre × R26-YFP–transgenic mice. (**a**) Expression of GFP and YFP by thymocytes stained for expression of CD4 and CD8, gated as CD4$^+$CD8$^+$ double-positive (DP) and individual CD4$^+$ SP (CD4SP) or CD8$^+$ SP (CD8SP) populations. Numbers in and adjacent to outlined areas indicate percent cells in each. (**b**) CD24 expression on CD4$^+$ SP populations with various expression of GFP and YFP, gated as in **a**. Numbers in plots indicate mean fluorescent intensity. (**c**) Expression of GFP and YFP by gated CD4$^+$ T cells from lymph nodes (LN) and spleen. Numbers in and adjacent to outlined areas indicate percent cells in each. (**d**) Methylation status of CpG motifs of the TSDR of the *Foxp3* locus in cells subcloned from purified GFP$^-$YFP$^-$, GFP$^+$YFP$^+$ and GFP$^-$YFP$^+$ cells. Numbers in and around chart indicate percent cells in each area. (**e**) GFP and YFP populations as a percentage of CD4$^+$ T cells in spleen, lymph nodes, liver and Peyer's patches of Foxp3-GFP-Cre × R26-YFP mice. Each symbol represents an individual mouse; small horizontal lines indicate the mean. Data are representative of four (**a**,**b**) or 20 (**c**) independent experiments with 6- to 9-week-old mice; are the average of results generated in three independent experiments (**d**); or are representative of three experiments (**e**).

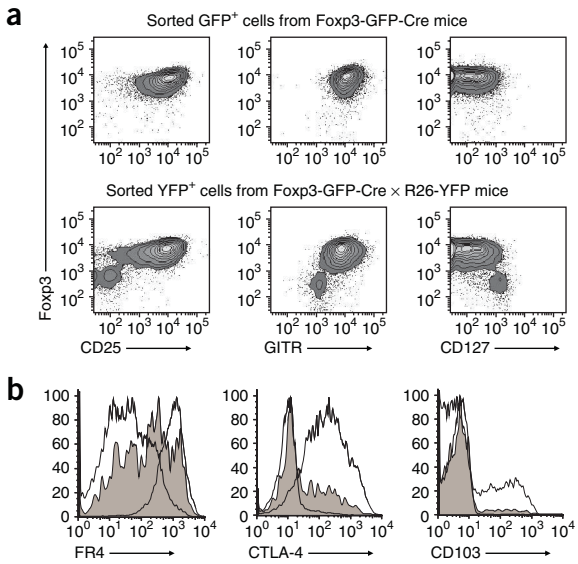

Figure 2 CD4$^+$ YFP$^+$ Foxp3$^-$ cells have a non–T_{reg} cell surface phenotype. (**a**) Cell surface staining of CD127, CD25 and GITR and sequential intracellular staining of Foxp3 in lymph node and spleen CD4$^+$ GFP$^+$ T cells purified by flow cytometry from Foxp3-GFP-Cre mice (top row) and CD4$^+$ YFP$^+$ T cells purified by sorting from Foxp3-GFP-Cre × R26-YFP mice (bottom row). (**b**) Cell surface staining of FR4 and CD103 and sequential intracellular staining of Foxp3 and CTLA-4 in lymph node and spleen T_{conv} cells (thick lines), YFP$^+$ Foxp3$^+$ T_{reg} cells (thin lines) and YFP$^+$ Foxp3$^-$ cells (filled histograms) from Foxp3-GFP-Cre × R26-YFP mice. Data are representative of three experiments with 6- to 9-week-old mice.

(**Fig. 1c**), which most probably represented newly generated aT_{reg} cells as a consequence of peripheral induction of Foxp3. Notably, analysis of the peripheral spleen and lymph node tissues showed that the GFP$^-$YFP$^+$ population accounted for up to 20% of the peripheral YFP$^+$ cells (**Fig. 1c**). To directly address the stability of the *Foxp3* locus in this newly identified population, we examined the methylation status of the T_{reg} cell–specific demethylated region (TSDR) of *Foxp3* in various T cell subsets[19]. Methylation of CpG islands in this region of the *Foxp3* locus is a principal control mechanism of *Foxp3* expression in mouse CD4$^+$ T cells, as 90% of the CpG sites in the examined intron of Foxp3$^-$ naive CD4$^+$ T cells are over 90% methylated, whereas the CpG sites in this intron are fully unmethylated in thymus-derived nT_{reg} cells and *in vivo*–generated aT_{reg} cells[20–22]. Bisulphite sequence analysis confirmed previous findings that 100% of CD4$^+$ GFP$^-$YFP$^-$ T_{conv} cells purified by flow cytometry sorting had over 85% CpG sites methylated, whereas less than 15% of the CpG sites were methylated in 90% of the T_{reg} cells (CD4$^+$ GFP$^+$YFP$^+$; **Fig. 1d** and **Supplementary Fig. 1**). In contrast, GFP$^-$YFP$^+$ cells purified by flow cytometry had a varied pattern of methylation status. Only 74% of the DNA strands had over 85% of the CpG sites in the TSDR methylated, which correlated positively with Foxp3 expression (**Supplementary Fig. 1**); 11% of the clones had over 85% of the CpG islands unmethylated and, most notably, 13% had partial methylation, with 15–85% of the CpG sites being unmethylated (**Fig. 1d**). Notably, there seemed to be a random pattern of partial methylation in the GFP$^-$YFP$^+$ cells (**Supplementary Fig. 1**), which suggested that factors that controlled the spontaneous loss of Foxp3 expression led to remethylation of the *Foxp3* locus in some cells. Alternatively, it was possible that a subset of GFP$^-$YFP$^+$ cells had never fully demethylated the locus even though they had expressed sufficient Foxp3 to 'turn on' the Cre enzyme. In this context, this methylation phenotype is reminiscent of what has been reported for *in vitro* transforming growth factor-β–induced T_{reg} cells[20].

Analysis of spleens, lymph nodes, livers and Peyer's patches of many mice showed that there were similar proportions of the various YFP$^+$ subsets throughout peripheral lymphoid compartments (**Fig. 1e**). Approximately 15% of the YFP$^+$ cells were negative for Foxp3 staining (**Fig. 2a**), which correlated with the proportion of YFP$^+$ cells that lacked GFP expression (**Fig. 1c**). These results suggested that a population of T cells existed in both the thymus and various lymphoid compartments that had expressed Foxp3 at one stage but ceased active translation of Foxp3 protein. We call the GFP$^-$YFP$^+$ cells 'exFoxp3 cells' here.

Next we examined the phenotype of the exFoxp3 cells in the periphery. The Foxp3$^-$ YFP$^+$ cells were uniformly CD25$^-$, with low expression of the immunomodulatory receptor GITR and high expression of CD127 (IL-7 receptor α-chain), differing considerably from the Foxp3$^+$ YFP$^+$ T_{reg} cells (**Fig. 2a**). Analysis of other cell surface molecules showed that the exFoxp3 cells had a mixed phenotype, with heterogeneous expression of 'signature' T_{reg} cell markers, including folate receptor 4 (FR4), cytotoxic T lymphocyte-associated antigen (CTLA-4) and CD103 (**Fig. 2b**). Previous Foxp3-knockout studies showed that ablation of Foxp3 *in vivo* and *ex vivo* resulted in the loss of the T_{reg} cell phenotypic 'signature'[9,10]; thus, the substantial alterations in the expression of CD25, GITR, CD127 and other surface markers in the GFP$^-$YFP$^+$ cells suggested similar instability had occurred in homeostatic conditions.

Activated-memory phenotype of exFoxp3 cells

Notably, the exFoxp3 cells did not represent a 'dead-end', terminally differentiated T_{reg} cell type but instead represented a cell type with plasticity that could develop an activated-memory cell phenotype, with heterogeneous CD62L expression and high CD44 expression (**Fig. 3a**). To directly assess if the exFoxp3 cells were effector-memory T cells, we sorted YFP$^+$ cells, stimulated them with phorbol 12-myristate 13-acetate (PMA) and ionomycin and examined intracellular cytokine production (**Fig. 3b–d**). A substantial percentage of the exFoxp3 cells produced interferon-γ (IFN-γ), which supported the hypothesis that these were indeed effector-memory T cells. Published studies have suggested a unique relationship between the differentiation of T_{reg} cells and that of IL-17-producing helper T cell on the basis of transcription factor plasticity during T cell differentiation, particularly in gut-associated lymphoid tissue[11,23]. Therefore, we examined the production of IL-17 by exFoxp3 cells isolated from gut-associated lymphoid tissue. A mean of 22.4% of exFoxp3 cells in Peyer's patches produced IL-17A, compared with a mean of 13.2% that produced IFN-γ (**Fig. 3c,d**). This contrasted with results obtained with other lymphoid tissues, in which the exFoxp3 cells had a T helper type 1–biased phenotype. For example, by flow cytometry, a mean of 32%, 31.7% or 11.2% of exFoxp3 cells isolated from the liver, spleen or lymph node, respectively, produced IFN-γ, but a much lower percentage of exFoxp3 cells in these tissues produced IL-17A (**Fig. 3c,d**). Together these results suggest that exFoxp3 populations contain effector-memory T cells with distinct cytokine-producing abilities depending on their microenvironment.

Autoimmune microenvironment favors loss of Foxp3

Lower Foxp3 expression in T_{reg} cells has been reported in various autoimmune diseases, including type 1 diabetes in nonobese diabetic (NOD) mice[1,3], a model of spontaneous autoimmune diabetes that shares many similarities with autoimmune type 1 diabetes in humans. Inflamed islets have a lower ratio of T_{reg} cells to T effector cells, which

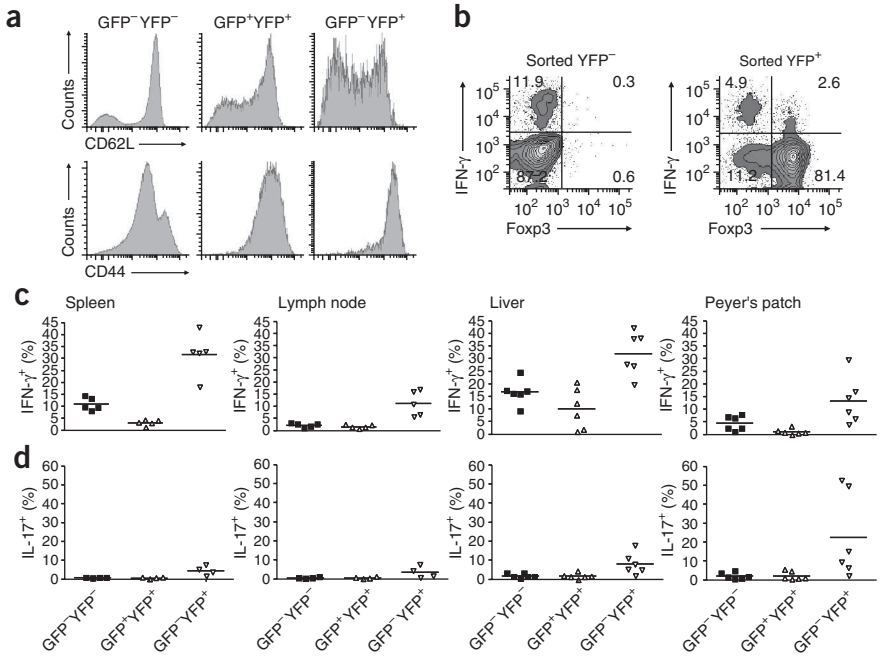

Figure 3 CD4$^+$ YFP$^+$ Foxp3$^-$ cells have a non–T_{reg}, memory cell surface phenotype and produce IFN-γ and IL-17. Analysis of peripheral lymphoid organ–resident CD4$^+$ GFP$^+$YFP$^+$, CD4$^+$ GFP$^-$YFP$^+$ and CD4$^+$ GFP$^-$YFP$^-$cells. (**a**) Expression of CD62L and CD44 by gated spleen CD4$^+$ populations. (**b**) Intracellular staining of Foxp3 and IFN-γ in purified spleen CD4$^+$ YFP$^+$ and CD4$^+$ YFP$^-$ T cells stimulated for 4 h with PMA, ionomycin and monensin. Numbers in quadrants indicate percent cells in each. (**c**,**d**) Frequency of GFP$^-$YFP$^-$, GFP$^+$YFP$^+$ and GFP$^-$YFP$^+$ populations that produce IFN-γ (**c**) or IL-17 (**d**). Each symbol represents an individual mouse; small horizontal lines indicate the mean. Data are representative of five (**a**,**b**) or three (**c**,**d**) independent experiments with 6- to 9-week-old mice.

is tightly associated with disease progression[1]. To test the hypothesis that the lower Foxp3 expression in autoimmune settings shifts the balance of T_{reg} cells to exFoxp3 cells, we crossed the Foxp3-GFP-Cre × R26-YFP mice onto the NOD strain and examined the proportion of CD4$^+$Foxp3$^+$ T_{reg} cells in aging, prediabetic Foxp3-GFP-Cre × R26-YFP NOD mice. We prepared infiltrates from the pancreases of 16- to 18-week-old mice and compared the abundance of the various GFP- and/or YFP-expressing populations in these infiltrates with those in draining pancreatic lymph nodes (PLNs) and nondraining inguinal lymph nodes (ILNs). Additionally, we analyzed the expression of markers of T_{reg} cells and memory-effector T cells. We found a significantly lower relative percentage of CD4$^+$ GFP$^+$YFP$^+$ T_{reg} cells in the CD4$^+$ YFP$^+$ T cell population in the pancreas than in PLNs or ILNs ($P < 0.03$; data not shown). In contrast, the percentage of GFP$^-$YFP$^+$ exFoxp3 cells was specifically higher in the pancreas (average 32.7%) than in ILNs and PLNs (average, 17.8% and 22.8%, respectively; **Fig. 4a**). Notably, exFoxp3 cells isolated from the pancreas had the lowest expression of CD25 and the highest expression of CD127 relative to that of exFoxp3 cells from the other compartments (**Fig. 4b**,**c**), and they produced IFN-γ (data not shown); these observations suggested that the autoimmune microenvironment altered T cell phenotypes and promoted pathogenicity. In addition, these results suggested that the appearance of the exFoxp3 cells was not simply a consequence of stochastic regulation of Foxp3 but instead was a consequence of antigen recognition in the inflamed setting.

To directly address the hypothesis proposed above, we further crossed the Foxp3-GFP-Cre × R26-YFP mice with BDC2.5 TCR–transgenic

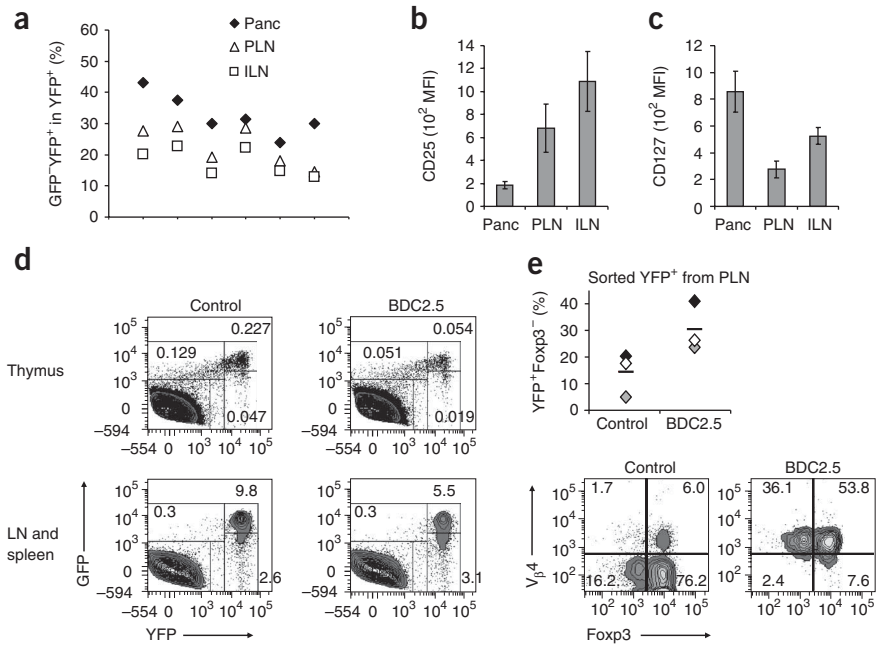

Figure 4 The autoimmune microenvironment favors loss of Foxp3 expression. (**a**) Frequency of GFP$^-$YFP$^+$ exFoxp3 cells among CD4$^+$YFP$^+$ cells in the pancreas (Panc), ILNs and PLNs of NOD mice. Each symbol indicates a different tissue (key); each vertical group represents an individual mouse. (**b**,**c**) Expression of CD25 (**b**) or CD127 (**c**) on exFoxp3 cells isolated from the pancreas, ILNs and PLNs, presented as mean fluorescence intensity (MFI). (**d**) Development of T_{reg} cells and exFoxp3 cells in BDC2.5 TCR–transgenic mice, assessed as expression of GFP and YFP in thymocytes, lymph node cells and splenocytes of 6- to 9-week-old BDC2.5 TCR–transgenic and control nontransgenic mice. Plots are gated on live thymocytes and enriched CD4$^+$ T cells from lymph node and spleen. Numbers in and adjacent to outlined areas indicate percent cells in each. (**e**) Expression of $V_\beta4$ (BDC2.5 TCR chain) and Foxp3 by CD4$^+$ YFP$^+$ T cells purified from PLNs of BDC2.5.TCR–transgenic or nontransgenic control mice. Top, each symbol represents an individual mouse and small horizontal lines indicate the mean; bottom, numbers in quadrants indicate percent cells in each. Data are pooled from two independent experiments (**a**), are representative of two independent experiments with six 16- to 18-week-old mice (**b**,**c**; error bars, s.d.) or are from three independent experiments with a total of three mice (**d**,**e**).

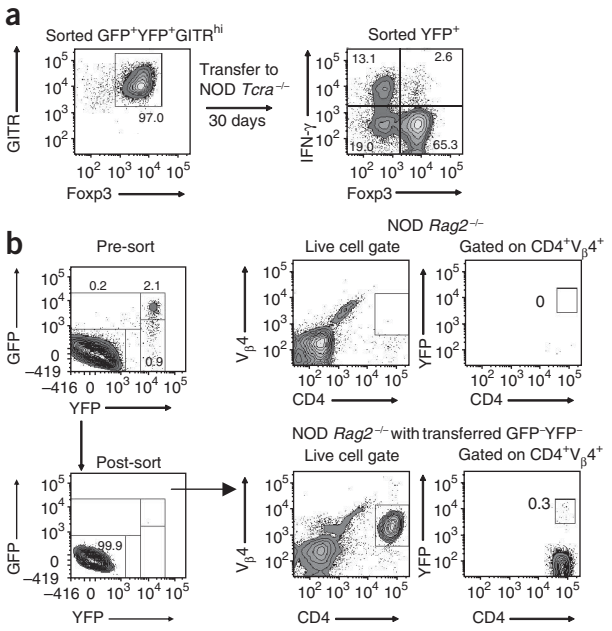

Figure 5 Development of exFoxp3 cells from T_{reg} cells after adoptive transfer. (**a**) Intracellular staining for Foxp3 and IFN-γ in YFP$^+$ cells from NOD *Tcra*$^{-/-}$ mice (right) given purified GFP$^+$YFP$^+$ GITR^{hi} BDC2.5 TCR–transgenic cells (left); 4 weeks after transfer, splenic YFP$^+$ cells were purified and exposed to PMA, ionomycin and monensin for 3–4 h before analysis. Number in bottom right corner indicates percent cells in outlined area above (left); numbers in quadrants indicate percent cells in each (right). Data are representative of three experiments with four mice. (**b**) Sort purification of GFP$^-$YFP$^-$ ILN cells from healthy BDC2.5 mice (left) for subsequent adoptive transfer into NOD *Rag2*$^{-/-}$ recipients, and expression of GFP and YFP by gated CD4$^+$ V$_\beta$4$^+$ pancreatic mononuclear cells obtained from acutely diabetic NOD *Rag2*$^{-/-}$ mice 7 d after transfer of the purified cells (bottom middle and right) and from control NOD *Rag2*$^{-/-}$ mice that did not receive cells (top middle and right). Data are representative of two experiments with three mice.

mice[24], whose TCR-transgenic CD4$^+$ T cells recognize a pancreatic islet autoantigen; this system allowed investigation of whether the expression of a pancreatic antigen–specific TCR would change the percentage of exFoxp3 cells and their pathogenic potential. The proportion of thymic CD4$^+$ SP T_{conv} and exFoxp3 cells was similar in control nontransgenic Foxp3-GFP-Cre × R26-YFP mice and BDC2.5 TCR–transgenic Foxp3-GFP-Cre × R26-YFP mice, although there were generally fewer thymic T_{reg} cells in the latter (**Fig. 4d**). However, there were up to twofold more exFoxp3 cells in the spleens and PLNs of the BDC2.5 TCR–transgenic mice than in those of their control littermates (**Fig. 4d,e**); this greater abundance was similar to the percentage found in the pancreas of conventional NOD mice. Together these data suggest that strong engagement of self antigen, especially in the inflammatory setting, can promote the generation of exFoxp3 cells.

Pathogenicity of exFoxp3 cells

To further test the hypothesis that established T_{reg} cells can be unstable and potentially pathogenic in an autoimmune setting, we sorted T_{reg} cells from Foxp3-GFP-Cre × R26-YFP BDC2.5 mice and transferred them into T cell–deficient NOD *Tcra*$^{-/-}$ mice (**Fig. 5a** and **Supplementary Fig. 2**). Analysis of the recipient mice 4 weeks after transfer of nT_{reg} cells showed that on average, a third of the cells (35.7%) had downregulated Foxp3, on the basis of the absence of expression of GFP or Foxp3 protein. Notably, these cells took on an effector-memory phenotype, with (on average) 28.4% of the GFP$^-$YFP$^+$ transgene-positive cells producing IFN-γ after stimulation with PMA and ionomycin (**Fig. 5a**). We did a similar experiment by transferring GFP$^-$YFP$^-$ transgene-positive cells into immunodeficient mice. In this study, about 0.5% of the transferred cells, all of which expressed the V$_\beta$4 chain of the BDC2.5 TCR transgene, 'turned on' YFP in the pancreas (**Fig. 5b**), indicative of transient Foxp3 expression. Together these results suggest that the exFoxp3 cells can be generated from nT_{reg} cell instability and/or abortive aT_{reg} cell induction dependent on interaction with self antigen. However, the aT_{reg} cell pathway did not seem to generate exFoxp3 cells efficiently *in vivo* after adoptive transfer.

To investigate the functional consequences of the exFoxp3 cells generated, we sorted the various subsets, including exFoxp3 cells, T_{conv} cells and T_{reg} cells, from CD4$^+$ cell–enriched lymph nodes and spleens of Foxp3-GFP-Cre × R26-YFP BDC2.5 mice and expanded each population *in vitro* with IL-2 and beads coated with antibody to CD3 (anti-CD3) plus anti-CD28 (ref. 25; **Fig. 6a**). The various T cell

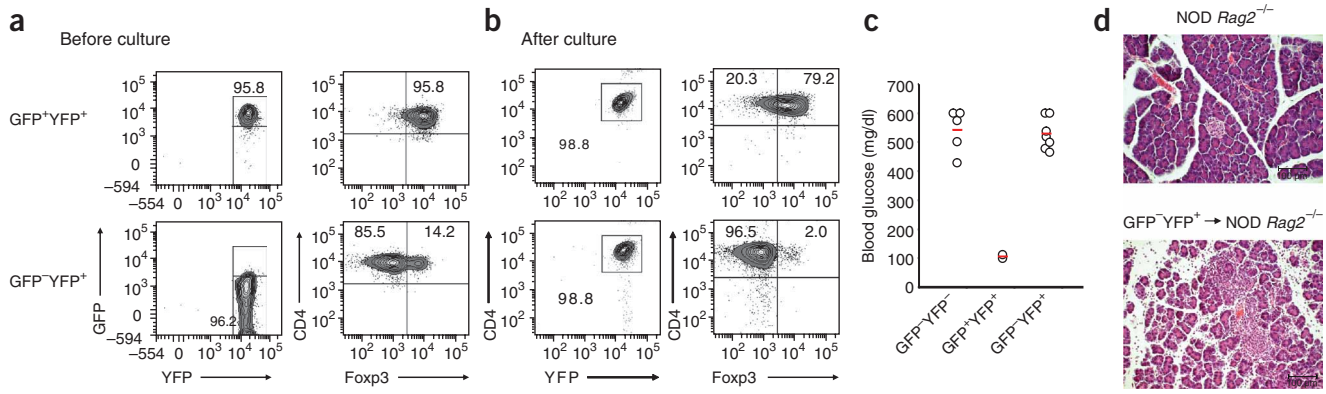

Figure 6 Pathogenicity of exFoxp3 cells. (**a**) Frequency of Foxp3$^+$ cells among CD4$^+$ T cells from Foxp3-GFP-Cre × R26-YFP BDC2.5 mice, sorted as GFP$^+$YFP$^+$ and GFP$^-$YFP$^+$ cells to a purity of over 95% and assessed by intracellular staining before culture. (**b**) Flow cytometry of purified cells cultured for 6–8 d with IL-2 plus beads coated with anti-CD3 and anti-CD28. Numbers in and adjacent to outlined areas and in quadrants indicate percent cells in each (**a**,**b**). (**c**) Blood glucose concentrations of NOD *Rag2*$^{-/-}$ mice given expanded populations of GFP$^-$YFP$^-$, GFP$^+$YFP$^+$ or GFP$^-$YFP$^+$ cells (5 × 10^5 cells), assessed on days 8–11 after transfer. Mice are considered diabetic when the blood glucose exceeds 250 mg/dl. Each symbol represents an individual mouse; small horizontal lines indicate the mean. (**d**) Hematoxylin and eosin staining of pancreas sections from NOD *Rag2*$^{-/-}$ mice that did not receive cells (top) or that received GFP$^-$YFP$^+$ cells 9 d before as described in **b** (bottom). Original magnification, ×200. Data are representative of three experiments (n = 4 mice in **d**).

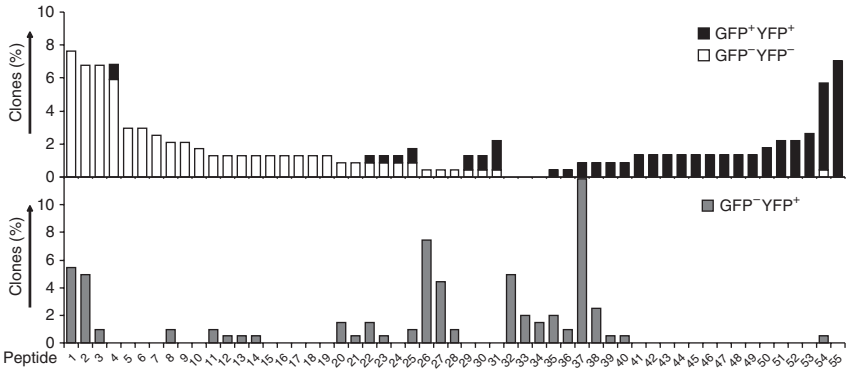

Figure 7 Development of exFoxp3 cells from both nT_{reg} cells and aT_{reg} cells. Frequency of unique CDR3 amino acid sequences (identified by peptide number along horizontal axis) in T_{conv} cells (GFP^-YFP^-; white bars), exFoxp3 cells (GFP^-YFP^+; gray bars) and T_{reg} cells (GFP^+YFP^+; black bars) sorted from BDC2.5 TCR–transgenic mice; cDNA was amplified with $V_\alpha 2$-specific primers and amplicons were subcloned and sequenced. Data are from two experiments (one mouse representative of two presented here).

subsets were stable throughout the 7–9 d in culture, as both the GFP^+YFP^+ T_{reg} cells and GFP^-YFP^+ exFoxp3 cells remained uniformly $CD4^+$ and YFP^+ and continued to have their respective high and low expression of GFP. Intracellular Foxp3 staining showed that less than 2% of the cells in the expanded GFP^-YFP^+ T cell population were $Foxp3^+$; although most cells in the expanded GFP^+YFP^+ population maintained expression of Foxp3, about 20% lost Foxp3 expression (**Fig. 6b**). We then transferred individually expanded populations of BDC2.5 TCR transgene–positive T_{reg} cells, exFoxp3 cells and T_{conv} cells into NOD recombinase-activating gene 2–deficient (*Rag2*$^{-/-}$) mice and monitored the development of autoimmune diabetes in the recipient mice. Mice that received GFP^+ YFP^+ T_{reg} cells had normal blood glucose concentrations (<250 mg/dl) throughout the study follow-up. In contrast, exFoxp3 cells, like T_{conv} cells, induced rapid islet destruction and the development of diabetes (**Fig. 6c,d**). Over 95% of the TCR-transgenic $CD4^+V_\beta 4^+$ cells expressed YFP (**Supplementary Fig. 3**), which indicated that the transferred exFoxp3 cells were responsible for the disease pathogenesis. These results suggest that exFoxp3 BDC2.5 cells function as effector T cells after recognition of pancreatic self antigen and induce rapid and severe type 1 diabetes.

Heterogeneous precursors of exFoxp3 cells

It was critical to address the ontogeny of the exFoxp3 cells directly, as it remained unclear whether in an unmanipulated setting the exFoxp3 cells arose from aborted $Foxp3^+$ aT_{reg} cells that had converted from T_{conv} cells in the periphery or resulted from the loss of Foxp3 expression in true $CD4^+Foxp3^+$ nT_{reg} cells. Published studies have suggested that rearrangement of endogenous TCRα chains and selective pressure during thymic development result in nT_{reg} cells having a unique TCR repertoire in the BDC2.5 mouse[26]. Thus, we isolated the various $CD4^+$ T cell subsets from Foxp3-GFP-Cre × R26-YFP BDC2.5 mice and then amplified, cloned and sequenced a region encompassing complementarity-determining region 3 (CDR3) through the constant region of the $V_\alpha 2$ TCR in these cells. Of 384 clones per subset, 227 T_{reg} cells, 202 exFoxp3 cells and 236 T_{conv} cells had productive V-gene and joining-gene rearrangements (**Supplementary Table 1**). As reported before[26], the endogenous TCR $V_\alpha 2$ repertoire of T_{reg} cells and T_{conv} cells from BDC2.5 TCR–transgenic mice was distinct, as only 12.8% of the CDR3 amino acid sequences of GFP^+YFP^+ T_{reg} cells were present in the GFP^-YFP^- T_{conv} cells (**Fig. 7**). The exFoxp3 cells shared CDR3 amino acid sequences with both T_{reg} cells and T_{conv} cells, overlapping 23.8% and 35.6%, respectively (**Fig. 7** and **Table 1**). Among the twelve most frequent CDR3 amino acid sequences found in the GFP^-YFP^+ cells (**Table 1**), four peptide sequences have been described before; CAAANSGTYQRF was dominant in T_{conv} cells, whereas CAASALRTGSWQLIF, CAASGAGGYKVVF and CAATHNNNRIFF were uniquely present in T_{reg} cells[26] (**Supplementary Table 2**). Given the broadness of the TCR repertoire, the number of sequenced clones from exFoxp3 cells was probably still relatively low; however, substantial overlap of the TCR repertoire with that of both T_{reg} cells and T_{conv} cells suggested exFoxp3 cells are heterogeneous, deriving in part from established T_{reg} cells that lost Foxp3 expression and in part from $Foxp3^-$ T_{conv} cells that expressed Foxp3, then lost Foxp3 expression after TCR engagement. As all the T_{conv} cells expressed a transgenic BDC2.5 TCR, it is plausible that interaction of the BDC2.5 TCR and an unknown islet antigen actually led to development of at least some of the exFoxp3 cells.

DISCUSSION

There has been controversy regarding the stability of T_{reg} cells in the periphery. It has been widely believed that T_{reg} cells represent a highly stable lineage in which few if any cells lose Foxp3 expression in normal homeostatic conditions. A small subset of $CD25^-Foxp3^+$ T_{reg} cells has been reported that is unstable and rapidly loses Foxp3 expression after transfer into a lymphopenic host[13,14]. Other studies have also suggested that T_{reg} cells can be unstable; however, these studies have been limited to *in vitro* culture or *in vivo* transfer to lymphopenic recipients. In this study, we have used a Foxp3 reporter lineage-marker system to demonstrate unequivocally that a subset of Foxp3-expressing cells indeed lost Foxp3 expression. The generation of the exFoxp3 cells was accelerated during the progression of autoimmune type 1 diabetes. These cells developed an effector-memory phenotype, produced pathogenic cytokines

Table 1 Most frequent CDR3 amino acid sequences in GFP^-YFP^+ cells

CDR3 sequence	J gene	GFP^-YFP^- 236[a]	GFP^+YFP^+ 227[a]	GFP^-YFP^+ 202[a]
CAARPRHNVLYF	TRAJ21*01	0.0%	0.9%	11.9%
CAASAGGGRALIF	TRAJ15*01	0.4%	0.0%	7.4%
CAAKKGYNVLYF	TRAJ21*01	7.6%	0.0%	5.4%
CAAANSGTYQRF	TRAJ13*01	6.8%	0.0%	5.0%
CAAKAHLGFASALTF	TRAJ35*02	0.0%	0.0%	5.0%
CAAKPGYNKLTF	TRAJ11*01	0.4%	0.0%	4.5%
CAASALRTGSWQLIF	TRAJ22*01	0.0%	0.9%	2.5%
CAASGAGGYKVVF	TRAJ12*01	0.0%	0.4%	2.0%
CAATHNNNRIFF	TRAJ31*02	0.0%	0.0%	2.0%
CAAKSGGSNYKLTF	TRAJ53*01	0.8%	0.4%	1.5%
CAAKKGYKLTF	TRAJ9*01	0.8%	0.0%	1.5%
CAATGNSAGNKLTF	TRAJ17*01	0.0%	0.0%	1.5%

Frequency of occurrence of the twelve most frequent CDR3 amino acid sequences in GFP^-YFP^- and GFP^+YFP^+ and GFP^-YFP^+ $CD4^+$ T cells populations, assessed as described in **Figure 7**. J gene, joining allele designation (International ImMunoGeneTics). [a]Total number of sequences.

and triggered the development of autoimmunity. Thus, Foxp3 expression is dynamically regulated in normal physiological conditions.

The paradigm in immunology is that autoimmunity is precipitated by an imbalance of pathogenic T cells and Foxp3$^+$ T_{reg} cells[27,28]. One dogma suggests that autoimmunity stems from a defect in T_{reg} cells that 'allows' pathogenic cells to escape regulation and mediate disease[29]. On the basis of our observations, we propose an alternative possibility: that Foxp3 instability can lead to the generation of pathogenic effector-memory T cells that promote autoimmunity. The efficiency of the T_{reg} cell system is a consequence of T_{reg} cell expression of a TCR repertoire biased toward self-recognition[18,30,31]. Thus, the frequency of precursors able to recognize self proteins is very high, and this facilitates efficient suppression. Moreover, T_{reg} cells have many functional properties that target dendritic cells, including both cell contact–dependent and soluble cytokine-specific suppressive activities[25]. These functional attributes allow this small subset to suppress local immunity through a combination of bystander suppression and infectious tolerance. However, these same attributes can backfire when a subset of the T_{reg} cells loses Foxp3 expression and turns into autoreactive effector cells. In the pancreas of NOD mice, the balance was shifted from Foxp3$^+$ T_{reg} cells to exFoxp3 cells. The exFoxp3 cells had very high expression of CD127, which is believed to be a direct Foxp3 target and represents a key marker of memory T cell subsets[10,32].

Although the detailed molecular mechanism of the generation of exFoxp3 cells still needs to be clarified, it is possible that during an autoimmune pathological T cell response, a functional deficiency of IL-2 signaling in the T_{reg} cells in the affected tissues may lead to a break in the positive feedback loop that controls Foxp3 stability, such that self-reactive T_{reg} cells may convert to effector cells with high diabetic potential. Consistent with that idea, we found specific enrichment for CD4$^+$Foxp3$^+$CD25$^-$ cells in the inflamed islet, which represents an unstable environment that favors the development of exFoxp3 cells, either through transient induction of Foxp3 in T_{conv} cells or loss of Foxp3 transcription in T_{reg} cells. Moreover, IL-2 treatment can efficiently restore the CD25 expression of intra-islet T_{reg} cells and protect mice from developing autoimmune diabetes[1]. Furthermore, it has been shown that T_{reg} cells depend on Dicer and therefore microRNA for proper function, and that exFoxp3 cell numbers are higher in Foxp3-specific Dicer-knockout mice[12]. Is has also been shown that the microRNA miR-155 modulates IL-2 signaling by targeting suppressor of cytokine signaling 1 (ref. 33) and that miR-155-deficient T_{reg} cells need higher IL-2 concentrations *in vitro* to achieve STAT5 phosphorylation similar to that in wild-type cells. Hence, it is possible that microRNA is involved in maintaining high Foxp3 expression in T_{reg} cells.

The lineage tracing through analysis of the endogenous V_α TCR use in BDC2.5 TCR–transgenic cell subsets showed that a considerable percentage of exFoxp3 cells shared ontogeny with both the Foxp3$^+$ T_{reg} lineage and T_{conv} lineage. It is likely that the same inflammatory autoimmune setting actually destabilizes both nT_{reg} cells and aT_{reg} cells. The aT_{reg} cells share many characteristics with nT_{reg} cells, including the fully unmethylated status of the TSDR in the *Foxp3* locus[19], similar cytokine expression and the T_{reg} cell mRNA expression 'fingerprint'. The aT_{reg} cells have a function complementary to that of nT_{reg} cells, particularly in response to self antigens not expressed in the thymus. Thus, it is possible that in inflammatory conditions, the development of aT_{reg} cells is aborted, allowing the self-reactive cells to develop directly into effector-memory T cells and promote autoimmune disease. Notably, the unexpected finding that transient Foxp3 expression favors the differentiation of RORγt$^+$ IL-17-producing T cells has been reported[34]. We speculate that in all cases, the molecular mechanism of destabilized Foxp3 involves epigenetic changes in the *Foxp3* locus in the inflamed site. In this context, one study has suggested that the IL-6 signaling pathway can remethylate a critical *Foxp3* CpG motif and suppress Foxp3 expression[35]. Other studies suggest that subsets of T_{reg} cells 'preferentially' and specifically suppress distinct helper T cell subset–mediated immune pathology. For instance, T_{reg} cell–specific ablation of the transcription factor IRF4 leads to impaired T helper type 2 suppression but normal T helper type 1 suppression[36]. In contrast, another study has reported that a subset of T_{reg} cells expressing the transcription factor T-bet suppresses T helper type 1 inflammation[37]. As T_{reg} cells and T_{conv} cells are closely related and share an mRNA and microRNA 'signature'[38], it is possible that some of this phenomenon is explained by T_{reg} cell–exFoxp3 cell pairs that are equipped with similar chemokine receptors to migrate to the same tissues and/or that some of the effectors are derived directly from T_{reg} cells in the inflamed tissues.

Finally, the plasticity of Foxp3 expression in the inflamed setting may also have implications in infectious diseases in which early inflammatory cytokines induced by the innate immune response may not only disable T_{reg} cells but also enhance immunity by creating a pathogenic autoreactive T cell repertoire locally in the infected tissues. This possibility may explain the commonly observed phenomenon of episodes of infections triggering autoimmune disease[39]. Thus, better understanding of the extracellular and intracellular signals that maintain or destabilize Foxp3 expression may have important therapeutic implications in a variety of disease settings ranging from autoimmunity to cancer and infectious disease.

METHODS

Methods and any associated references are available in the online version of the paper at http://www.nature.com/natureimmunology/.

Accession code. UCSD-Nature Signaling Gateway (http://www.signaling-gateway.org): A002750.

Note: Supplementary information is available on the Nature Immunology website.

ACKNOWLEDGMENTS

We thank C.J. McArthur, M. Lee, N. Grewal, S. Jiang, J. Beilke and S. Zhu for technical assistance; N. Martinier and D. Fuentes for animal husbandry; and A. Abbas, Q. Tang, M. Anderson, R. Locksley and members of the Bluestone laboratory for discussions and reading the manuscript. Supported by the US National Institutes of Health (P01 AI35297 and U19 AI056388 to J.A.B., and P30 DK63720 for core support), the American Diabetes Association (X.Z.), the Swiss National Science Foundation (PBBSB-118644 to L.T.J.), the Roche Research Foundation (L.T.J.), the Novartis Foundation (formerly Ciba-Geigy Jubilee Foundation; L.T.J.) and the US National Institute of General Medical Sciences (1 R25 GM56847 to C.P.).

AUTHOR CONTRIBUTIONS

X.Z. and J.A.B. initiated the study; X.Z., S.L.B.-B. and L.T.J. designed and did experiments, analyzed data and wrote the manuscript; C.P. and M.M.-L. designed and did experiments; M.A. did bioinformatic analysis of TCR sequences with help from X.Z., S.L.B.-B. and M.N.; M.N. and W.R. did experiments; and J.A.B. designed experiments, supervised the work, analyzed data and wrote the manuscript.

Published online at http://www.nature.com/natureimmunology/.
Reprints and permissions information is available online at http://npg.nature.com/reprintsandpermissions/.

1. Tang, Q. *et al.* Central role of defective interleukin-2 production in the triggering of islet autoimmune destruction. *Immunity* **28**, 687–697 (2008).
2. Bluestone, J.A., Tang, Q. & Sedwick, C.E. T regulatory cells in autoimmune diabetes: past challenges, future prospects. *J. Clin. Immunol.* **28**, 677–684 (2008).
3. Wan, Y.Y. & Flavell, R.A. Regulatory T-cell functions are subverted and converted owing to attenuated Foxp3 expression. *Nature* **445**, 766–770 (2007).

4. Hori, S., Nomura, T. & Sakaguchi, S. Control of regulatory T cell development by the transcription factor Foxp3. *Science* **299**, 1057–1061 (2003).
5. Bennett, C.L. & Ochs, H.D. IPEX is a unique X-linked syndrome characterized by immune dysfunction, polyendocrinopathy, enteropathy, and a variety of autoimmune phenomena. *Curr. Opin. Pediatr.* **13**, 533–538 (2001).
6. Bennett, C.L. *et al.* The immune dysregulation, polyendocrinopathy, enteropathy, X-linked syndrome (IPEX) is caused by mutations of *FOXP3*. *Nat. Genet.* **27**, 20–21 (2001).
7. Brunkow, M.E. *et al.* Disruption of a new forkhead/winged-helix protein, scurfin, results in the fatal lymphoproliferative disorder of the scurfy mouse. *Nat. Genet.* **27**, 68–73 (2001).
8. Bluestone, J.A. & Abbas, A.K. Natural versus adaptive regulatory T cells. *Nat. Rev. Immunol.* **3**, 253–257 (2003).
9. Gavin, M.A. *et al.* Foxp3-dependent programme of regulatory T-cell differentiation. *Nature* **445**, 771–775 (2007).
10. Williams, L.M. & Rudensky, A.Y. Maintenance of the Foxp3-dependent developmental program in mature regulatory T cells requires continued expression of Foxp3. *Nat. Immunol.* **8**, 277–284 (2007).
11. Yang, X.O. *et al.* Molecular antagonism and plasticity of regulatory and inflammatory T cell programs. *Immunity* **29**, 44–56 (2008).
12. Zhou, X. *et al.* Selective miRNA disruption in T reg cells leads to uncontrolled autoimmunity. *J. Exp. Med.* **205**, 1983–1991 (2008).
13. Komatsu, N. *et al.* Heterogeneity of natural Foxp3$^+$ T cells: a committed regulatory T-cell lineage and an uncommitted minor population retaining plasticity. *Proc. Natl. Acad. Sci. USA* **106**, 1903–1908 (2009).
14. Tsuji, M. *et al.* Preferential generation of follicular B helper T cells from Foxp3$^+$ T cells in gut Peyer's patches. *Science* **323**, 1488–1492 (2009).
15. Srinivas, S. *et al.* Cre reporter strains produced by targeted insertion of EYFP and ECFP into the ROSA26 locus. *BMC Dev. Biol.* **1**, 4 (2001).
16. Fontenot, J.D. *et al.* Regulatory T cell lineage specification by the forkhead transcription factor foxp3. *Immunity* **22**, 329–341 (2005).
17. Kishimoto, H. & Sprent, J. The thymus and negative selection. *Immunol. Res.* **21**, 315–323 (2000).
18. Jordan, M.S. *et al.* Thymic selection of CD4$^+$CD25$^+$ regulatory T cells induced by an agonist self-peptide. *Nat. Immunol.* **2**, 301–306 (2001).
19. Huehn, J., Polansky, J.K. & Hamann, A. Epigenetic control of FOXP3 expression: the key to a stable regulatory T-cell lineage? *Nat. Rev. Immunol.* **9**, 83–89 (2009).
20. Floess, S. *et al.* Epigenetic control of the foxp3 locus in regulatory T cells. *PLoS Biol.* **5**, e38 (2007).
21. Kim, H.P. & Leonard, W.J. CREB/ATF-dependent T cell receptor-induced FoxP3 gene expression: a role for DNA methylation. *J. Exp. Med.* **204**, 1543–1551 (2007).
22. Polansky, J.K. *et al.* DNA methylation controls Foxp3 gene expression. *Eur. J. Immunol.* **38**, 1654–1663 (2008).
23. Zhou, L. *et al.* TGF-β-induced Foxp3 inhibits T_H17 cell differentiation by antagonizing RORγt function. *Nature* **453**, 236–240 (2008).
24. Katz, J.D., Wang, B., Haskins, K., Benoist, C. & Mathis, D. Following a diabetogenic T cell from genesis through pathogenesis. *Cell* **74**, 1089–1100 (1993).
25. Tang, Q. *et al.* In vitro-expanded antigen-specific regulatory T cells suppress autoimmune diabetes. *J. Exp. Med.* **199**, 1455–1465 (2004).
26. Wong, J., Mathis, D. & Benoist, C. TCR-based lineage tracing: no evidence for conversion of conventional into regulatory T cells in response to a natural self-antigen in pancreatic islets. *J. Exp. Med.* **204**, 2039–2045 (2007).
27. Tang, Q. & Bluestone, J.A. The Foxp3$^+$ regulatory T cell: a jack of all trades, master of regulation. *Nat. Immunol.* **9**, 239–244 (2008).
28. Salomon, B. *et al.* B7/CD28 costimulation is essential for the homeostasis of the CD4$^+$CD25$^+$ immunoregulatory T cells that control autoimmune diabetes. *Immunity* **12**, 431–440 (2000).
29. Sakaguchi, S. *et al.* Foxp3$^+$CD25$^+$CD4$^+$ natural regulatory T cells in dominant self-tolerance and autoimmune disease. *Immunol. Rev.* **212**, 8–27 (2006).
30. Hsieh, C.S., Zheng, Y., Liang, Y., Fontenot, J.D. & Rudensky, A.Y. An intersection between the self-reactive regulatory and nonregulatory T cell receptor repertoires. *Nat. Immunol.* **7**, 401–410 (2006).
31. Hsieh, C.S. & Rudensky, A.Y. The role of TCR specificity in naturally arising CD25$^+$CD4$^+$ regulatory T cell biology. *Curr. Top. Microbiol. Immunol.* **293**, 25–42 (2005).
32. Liu, W. *et al.* CD127 expression inversely correlates with FoxP3 and suppressive function of human CD4$^+$ T reg cells. *J. Exp. Med.* **203**, 1701–1711 (2006).
33. Lu, L.F. *et al.* Foxp3-dependent microRNA155 confers competitive fitness to regulatory T cells by targeting SOCS1 protein. *Immunity* **30**, 80–91 (2009).
34. Lochner, M. *et al.* In vivo equilibrium of proinflammatory IL-17$^+$ and regulatory IL-10$^+$Foxp3$^+$RORγt$^+$ T cells. *J. Exp. Med.* **205**, 1381–1393 (2008).
35. Lal, G. *et al.* Epigenetic regulation of Foxp3 expression in regulatory T cells by DNA methylation. *J. Immunol.* **182**, 259–273 (2009).
36. Zheng, Y. *et al.* Regulatory T-cell suppressor program co-opts transcription factor IRF4 to control T_H2 responses. *Nature* **458**, 351–356 (2009).
37. Koch, M.A. *et al.* The transcription factor T-bet controls regulatory T cell homeostasis and function during type 1 inflammation. *Nat. Immunol.* **10**, 595–602 (2009).
38. Cobb, B.S. *et al.* A role for Dicer in immune regulation. *J. Exp. Med.* **203**, 2519–2527 (2006).
39. Rose, N.R. The adjuvant effect in infection and autoimmunity. *Clin. Rev. Allergy Immunol.* **34**, 279–282 (2008).

ONLINE METHODS

Mice. NOD.BDC2.5, Foxp3-GFP-Cre and Rosa26-loxP-Stop-loxP-YFP reporter mice have been described[12,15,24]. All mice were housed and bred in specific pathogen–free conditions in the Animal Barrier Facility of the University of California, San Francisco. All animal experiments were approved by the Institutional Animal Care and Use Committee of the University of California, San Francisco.

Antibodies. Labeled anti-CD4 (RM4-5), anti-CD8 (Ly-2), anti-CD25 (PC61), anti-CD44 (pgp-1), anti-GITR (DTA-1), anti-CD62L (MEL14), anti-CD103 (M290), anti-CD127 (A7R34), anti-CD152 (UC10-4F10), anti-Foxp3 (FJK-16s), anti-FR4 (eBio12A5), anti-$V_\beta4$ (KT4), anti-IL-17A (eBio17B7) and anti-IFN-γ (XMG1.2) and specific isotype-matched control antibodies were from BD PharMingen or eBioscience. Anti-CD24 (91) was from Southern Biotechnology Associates.

Flow cytometry. For cytokine analysis, cells were incubated for 3–4 h at 37 °C with 0.5 μM ionomycin, 10 ng/ml of PMA and 3 μM monensin before being fixed and made permeable (Foxp3 Staining kit; eBioscience) and were stained for intracellular proteins. Stained cells were analyzed with a FACSCalibur and CELLQuest software or an LSR II and FACSDiva (BD Biosciences). T cells were sorted with a MoFlo high-speed cell sorter (DakoCytomation) or FACSAria (BD Biosciences). For discrimination of GFP versus YFP signals, 510-nm/20-nm filters (495LP dichroic mirror) and 560-nm/40-nm filters (535LP dichroic mirror) were used.

***In vitro* population expansion and *in vivo* transfer of T cells.** Sorted T cells were stimulated with anti-CD3 and anti-CD28 Dynabeads (Invitrogen) at a cell/bead ratio of 1:1, supplemented with recombinant human IL-2 (2,000 IU/ml) in complete medium (DMEM containing 10% (vol/vol) heat-inactivated FBS (Biosource International), nonessential amino acids, 0.5 mM sodium pyruvate, 5 mM HEPES, pH 7.4, 1 mM GlutaMAX I (all from Invitrogen) and 55 μM β-mercaptoethanol (Sigma-Aldrich)). Cultures were monitored daily and were maintained for 7–9 d at a density of 0.7×10^6 to 1×10^6 cells per ml by dilution with IL-2-supplemented complete medium. At the end of culture, beads coated with anti-CD3 and anti-CD28 were removed by centrifugation on Ficoll. Then, 0.5×10^6 to 1×10^6 cells were transferred intravenously into NOD *Rag2*$^{-/-}$ or NOD *Tcra*$^{-/-}$ mice. Blood glucose concentrations were measured with an Accu-Chek glucose meter (Roche).

***Foxp3* methylation analysis.** Sort-purified cells were assessed by bisulphite sequence analysis[21]. Methylation-specific PCR primer sequences were 5′-TATT TTTTTGGGTTTTGGGATATTA-3′ (forward) and 5′-AACCAACCAACTTCCT ACACTATCTAT-3′ (reverse).

TCR repertoire analysis. YFP$^-$GFP$^-$, YFP$^+$GFP$^-$ and YFP$^+$GFP$^+$ $V_\alpha2$ TCR clones (384 each) were sequenced by McLab. A Python script was used for extraction of full-length sequences, which were then trimmed to include only the PCR-amplified TCR $V_\alpha2$ domains. Sequences were submitted by batch to the International Immunogenetics Information System website for V-gene and joining-gene analysis. Of the original 384 clones per cell population, 227 T_{reg} cells, 202 YFP$^+$GFP$^-$ cells and 236 T_{conv} cells had productive V- and joining-gene rearrangements. A separate script was used for compilation of occurrences of each oligonucleotide and CDR3 peptide sequence in each cell population and for comparison of occurrences among the three populations.

Isolation of lymphocytes from pancreas. Pancreases were excised independently of lymph nodes and were incubated for 30 min at 37 °C in collagenase P (1 mg/ml; Roche), DNase (20 μg/ml) and 0.2% (wt/vol) BSA in RPMI medium. Digested tissue was strained through a 70-μM cell strainer (BD Biosciences) and was washed once with RPMI medium containing DNase. Lymphocytes were separated from low-density pancreatic cells by centrifugation through a 40%–60% (vol/vol) percoll gradient. Lymphocytes were washed and stained for flow cytometry.

doi:10.1038/ni.1774

Foxp3 instability leads to the generation of pathogenic memory T cells *in vivo*

Xuyu Zhou, Samantha Bailey-Bucktrout, Lukas T. Jeker, Cristina Penaranda, Marc Martínez-Llordella, Meredith Ashby, Maki Nakayama, Wendy Rosenthal & Jeffrey A. Bluestone

Supplementary material legends

Supplementary Fig. 1. Methylation analysis of the *Foxp3* locus. (A) $CD4^+$ populations were sorted from the LN and spleen of male mice. Post sort analysis of GFP vs. YFP (top row) and CD4 vs Foxp3 intracellular staining. **(B)** Schematic of the *Foxp3* locus showing the TSDR amplified for CpG methylation analysis. The TATA box of the promoter is indicated, and Amp represents the region analyzed by bisulphite treatment, amplification and sequencing. The positions of the CpG motifs in this region are indicated. –2 and –1 are the non-coding exons upstream of exon 1 (filled box) **(C)** The methylation status of the CpG motifs in up to 20 DNA strands subcloned from purified T_{conv}, T_{reg} and exFoxp3 cells. Each row represents a DNA strand and each box represents the CpG motif as indicated. Filled box; methylated, open box; un-methylated.

Supplementary Fig. 2. Foxp3 instability *in vivo*. The GFP^+YFP^+ $GITR^{high}$ cells described in Fig. 5 were transferred into NOD *Tcra*$^{-/-}$ mice; four weeks later, transferred YFP^+ cells were purified and Foxp3 expression were determined by using intracellular staining. 3 mice are shown.

Supplementary Fig. 3. Pathogenic cells causing T1D are YFP^+. Splenocytes from the diabetic mice described in **Fig. 6C** were analyzed by flow cytometry. Representative of 4 mice.

Supplementary Table 1. CDR3 and $V_\alpha 2$ subclass expression in $CD4^+$ T cell subsets in Foxp3-GFP-Cre x R26-YFP BDC2.5 TCR Tg^+ mice. Subsets were sort purified from LN and spleen of Foxp3-GFP-Cre x R26-YFP BDC2.5 TCR Tg^+ mice, and the $V_\alpha 2$ CDR3, V and J sequences were determined. The predicted amino acid sequence was determined through use of the IMGT database. Numbers of obtained sequences in each population are indicated. The clone number refers to the graphical data in **Fig. 7**.

Supplementary Table 2. Comparison of CDR3 sequences with the study described in ref. 24. Productive CDR3 amino acid sequences obtained from peripheral $CD4^+$ T_{reg} ($Foxp3^+GFP^+$ YFP^+), exT_{reg} ($Foxp3^-GFP^-$ YFP^+), and T_{conv} ($Foxp3^-GFP^-$ YFP^-) from Foxp3-GFP-Cre x R26-YFP BDC2.5 TCR Tg^+ mice were compared with CDR3 amino acid (a.a.) sequences of T_{reg} (Tr) and T_{conv} (Tc) from the indicated organs of BDC2.5 TCR Tg mice published previously[24] . The most frequent cell population for any individual CDR3 a.a. sequence, in each experiment, is highlighted in bold.

Supplementary Figure 1

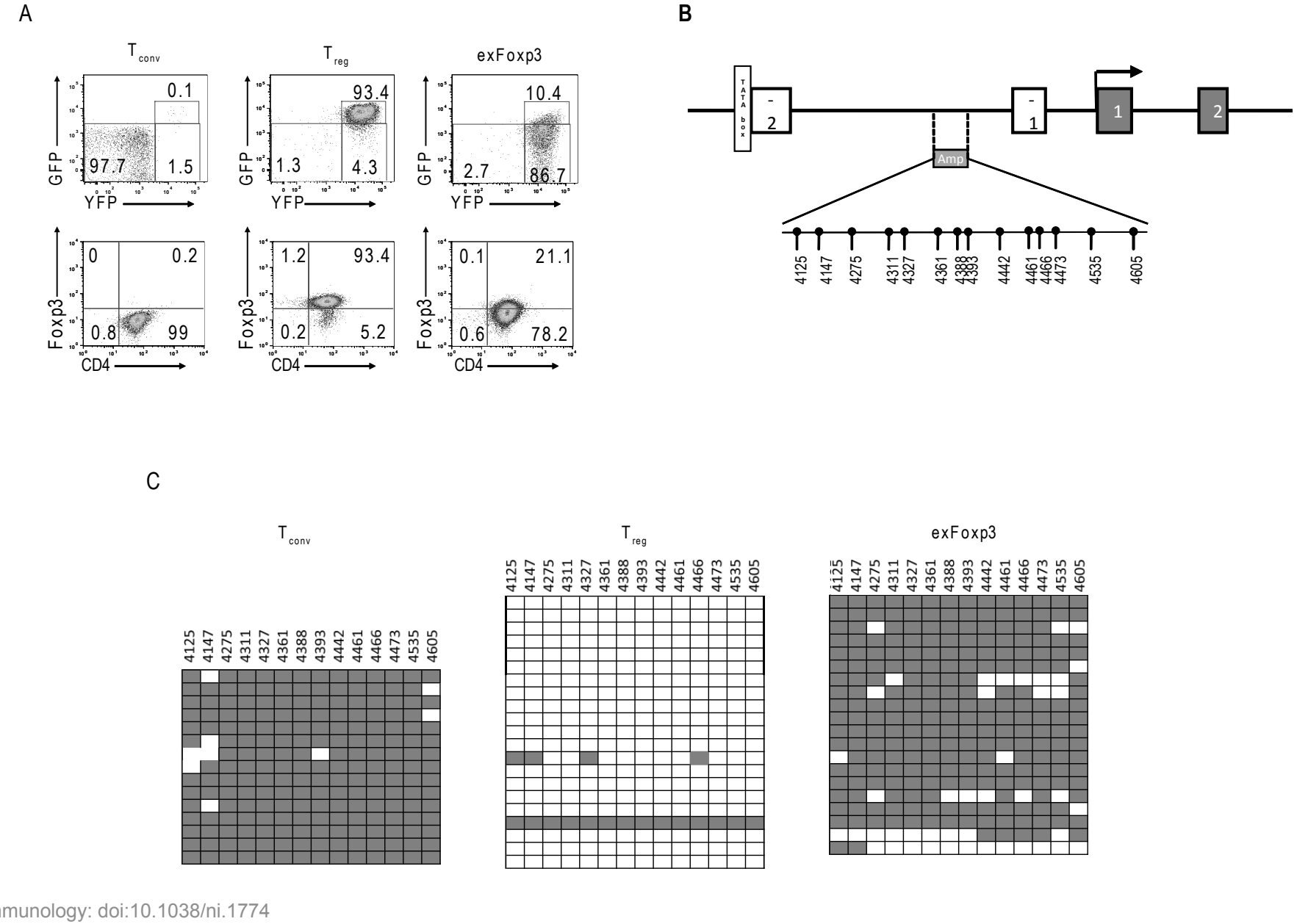

Supplementary Figure2

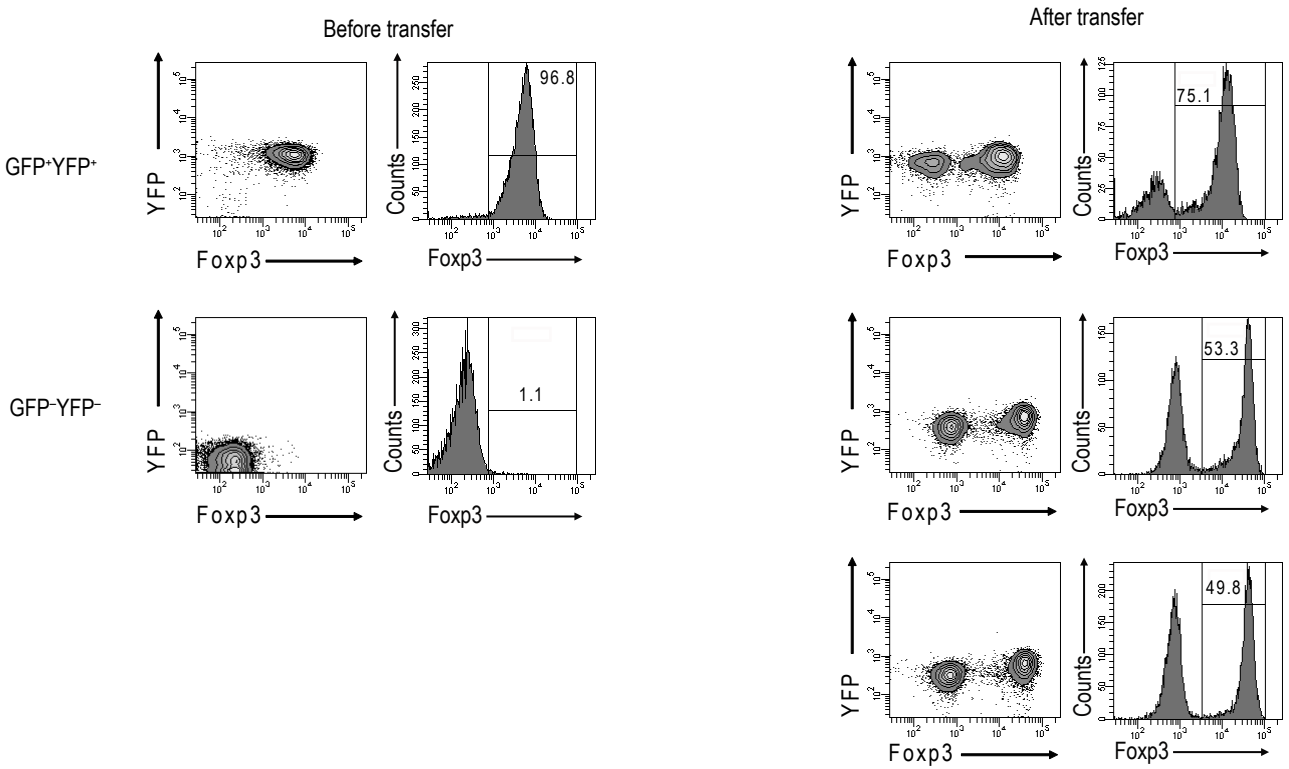

Nature Immunology: doi:10.1038/ni.1774

Supplementary Figure3

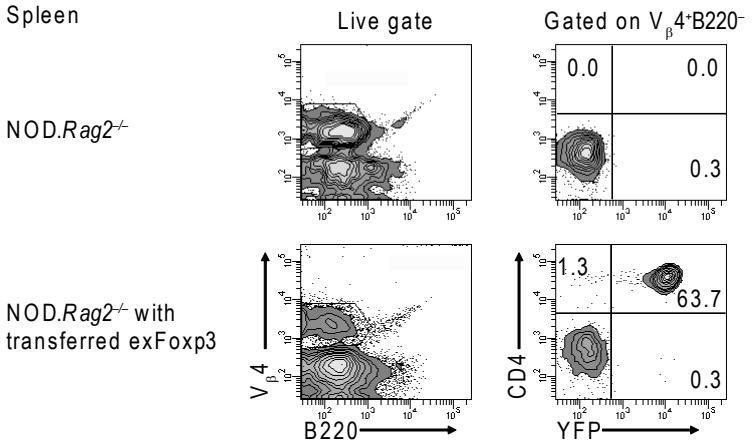

Supplementary Table 1. CDR3 and $V_\alpha 2$ subclass expression in $CD4^+$ T cell subsets.

clone	peptide	J gene	T_{reg}	exFoxp3	T_{conv}
1	CAAKKGYNVLYF	TRAJ21*01	0	11	18
2	CAAANSGTYQRF	TRAJ13*01	0	10	16
3	CAASNSGTYQRF	TRAJ13*01	0	2	16
4	CAASGQGGRALIF	TRAJ15*01	2	0	14
5	CAAASSGSWQLIF	TRAJ22*01	0	0	7
6	CAASAIGLGYKLTF	TRAJ9*01	0	0	7
7	CAASAQGGRALIF	TRAJ15*01	0	0	6
8	CAASYNNNRIFF	TRAJ31*02	0	2	5
9	CAASSTGGNNKLTF	TRAJ56*01	0	0	5
10	CAATGQGGRALIF	TRAJ15*01	0	0	4
11	CAAKGTNYNVLYF	TRAJ21*01	0	2	3
12	CAATYGNEKITF	TRAJ48*01	0	1	3
13	CAATRGSALGRLHF	TRAJ18*01	0	1	3
14	CAASYGNEKITF	TRAJ48*01	0	1	3
15	CAASKGNTRKLIF	TRAJ37*01	0	0	3
16	CAASSSGSWQLIF	TRAJ22*01	0	0	3
17	CAAKVVGQLTF	TRAJ5*01	0	0	3
18	CAASVTGGNNKLTF	TRAJ56*01	0	0	3
19	CAARSDRGSALGRLHF	TRAJ18*01	0	0	3
20	CAAKKGYKLTF	TRAJ9*01	0	3	2
21	CAVANSGTYQRF	TRAJ13*01	0	1	2
22	CAAKSGGSNYKLTF	TRAJ53*01	1	3	2
23	CAASGTGGYKVVF	TRAJ12*01	1	1	2
24	CAASHQGGRALIF	TRAJ15*01	1	0	2
25	CAAKGTTGNTRKLIF	TRAJ37*01	2	2	2
26	CAASAGGGRALIF	TRAJ15*01	0	15	1
27	CAAKPGYNKLTF	TRAJ11*01	0	9	1
28	CAASAGNMGYKLTF	TRAJ9*01	0	2	1
29	CAARPNYNVLYF	TRAJ21*01	2	0	1
30	CAAHQGGRALIF	TRAJ15*01	2	0	1
31	CAASGKGGRALIF	TRAJ15*01	4	0	1
32	CAAKAHLGFASALTF	TRAJ35*02	0	10	0
33	CAATHNNNRIFF	TRAJ31*02	0	4	0
34	CAATGNSAGNKLTF	TRAJ17*01	0	3	0
35	CAASGAGGYKVVF	TRAJ12*01	1	4	0
36	CAASPTNTGKLTF	TRAJ27*01	1	2	0
37	CAARPRHNVLYF	TRAJ21*01	2	24	0
38	CAASALRTGSWQLIF	TRAJ22*01	2	5	0
39	CAAKGGYKVVF	TRAJ12*01	2	1	0
40	CAAKGTGGYKVVF	TRAJ12*01	2	1	0
41	CAASIVGRALIF	TRAJ15*01	3	0	0
42	CAASGVRDMGYKLTF	TRAJ9*01	3	0	0
43	CAAKDQGGRALIF	TRAJ15*01	3	0	0
44	CAAMGAGANTGKLTF	TRAJ52*01	3	0	0
45	CAASATGGYKVVF	TRAJ12*01	3	0	0
46	CAASSPRGSWQLIF	TRAJ22*01	3	0	0
47	CAGTNAYKVIF	TRAJ30*01	3	0	0
48	CAARDMGYKLTF	TRAJ9*01	3	0	0
49	CAAKGRGSALGRLHF	TRAJ18*01	3	0	0
50	CAASKSGTYQRF	TRAJ13*01	4	0	0
51	CAATGGYKVVF	TRAJ12*01	5	0	0
52	CAATFASALTF	TRAJ35*02	5	0	0
53	CAASANSRALIF	TRAJ15*01	6	0	0
54	CAASANSGTYQRF	TRAJ13*01	12	1	1
55	CAAGQGGRALIF	TRAJ15*01	16	0	0

Supplementary Table 2. Comparison of CDR3 sequences found in this study with the study described in ref. 24

	Current study			**Ref. 24**									
CDR3 AA seq	**T_{reg}**	**exFoxp3**	**T_{conv}**	Thy Tr	Thy Tc	LN Tr	LN Tc	PLN Tr	PLN Tc	Panc Tr	Panc Tc	**T_{reg}**	**T_{con}**
CAAANSGTYQRF	0	10	**16**		11		8	1	9		8	1	**36**
CAASALRTGSWQLIF	2	**5**	0							1		**1**	0
CAASGAGGYKVVF	1	**4**	0					1				**1**	0
CAATHNNNRIFF	0	**4**	0					1				**1**	0
CAASEAGGYKVVF	0	**2**	0					1				**1**	0
CAASPFRTGNTRKLIF	0	**2**	0			1						**1**	0
CAASWNYAQGLTF	0	**2**	0		1	3		1				**4**	1
CAASYNNNRIFF	0	2	**5**		11		26		19		11	0	**67**
CAAAYGNEKITF	0	**1**	0						1			0	**1**
CAAFYQGGRALIF	0	**1**	0			1						**1**	0
CAAGYGNEKITF	0	**1**	**1**		3				2		2	0	**7**
CAAPNNNNRIFF	0	**1**	0		4		5		2			0	**11**
CAASAEGANTGKLTF	0	**1**	**1**				1		2			0	**3**
CAASANSGTYQRF	**12**	1	1	10		11		7		17		**35**	0
CAASATGGNNKLTF	0	**1**	0					1				**1**	0
CAASKNSGTYQRF	0	**1**	**1**			1						**1**	0
CAASKSADRLTF	0	**1**	0		1							0	**1**
CAASNNNNRIFF	0	**1**	0				1					0	**1**
CAASQTGGNNKLTF	0	**1**	0							1		**1**	0
CAASRVYNQGKLIF	0	**1**	0				1	1				1	1
CAASYGNEKITF	0	1	**3**		10		10	1	11		8	1	**39**
CAATASLGKLQF	**1**	**1**	0	1				1		2		**3**	0
CAATSSGQKLVF	0	**1**	0	3		2						**2**	0
CAATYGNEKITF	0	1	**3**		7		4		3		2	0	**16**
CAVANSGTYQRF	0	1	**2**								2	0	**2**

Mice.

NOD.BDC2.5, Foxp3-GFP-Cre and Rosa26-loxP-Stop-loxP-YFP reporter mice have been described12, 15, 24. All mice were housed and bred in specific pathogen–free conditions in the Animal Barrier Facility of the University of California, San Francisco. All animal experiments were approved by the Institutional Animal Care and Use Committee of the University of California, San Francisco.

Antibodies.

Labeled anti-CD4 (RM4-5), anti-CD8 (Ly-2), anti-CD25 (PC61), anti-CD44 (pgp-1), anti-GITR (DTA-1), anti-CD62L (MEL14), anti-CD103 (M290), anti-CD127 (A7R34), anti-CD152 (UC10-4F10), anti-Foxp3 (FJK-16s), anti-FR4 (eBio12A5), anti-Vbeta4 (KT4), anti-IL-17A (eBio17B7) and anti-IFN-gamma (XMG1.2) and specific isotype-matched control antibodies were from BD PharMingen or eBioscience. Anti-CD24 (91) was from Southern Biotechnology Associates.

Flow cytometry.

For cytokine analysis, cells were incubated for 3–4 h at 37 °C with 0.5 muM ionomycin, 10 ng/ml of PMA and 3 muM monensin before being fixed and made permeable (Foxp3 Staining kit; eBioscience) and were stained for intracellular proteins. Stained cells were analyzed with a FACSCalibur and CELLQuest software or an LSR II and FACSDiva (BD Biosciences). T cells were sorted with a MoFlo high-speed cell sorter (DakoCytomation) or FACSAria (BD Biosciences). For discrimination of GFP versus YFP signals, 510-nm/20-nm filters (495LP dichroic mirror) and 560-nm/40-nm filters (535LP dichroic mirror) were used.

In vitro population expansion and in vivo transfer of T cells.

Sorted T cells were stimulated with anti-CD3 and anti-CD28 Dynabeads (Invitrogen) at a cell/bead ratio of 1:1, supplemented with recombinant human IL-2 (2,000 IU/ml) in complete medium (DMEM containing 10% (vol/vol) heat-inactivated FBS (Biosource International), nonessential amino acids, 0.5 mM sodium pyruvate, 5 mM HEPES, pH 7.4, 1 mM GlutaMAX I (all from Invitrogen) and 55 muM beta-mercaptoethanol (Sigma-Aldrich)). Cultures were monitored daily and were maintained for 7–9 d at a density of 0.7 times 106 to 1 times 106 cells per ml by dilution with IL-2-supplemented complete medium. At the end of culture, beads coated with anti-CD3 and anti-CD28 were removed by centrifugation on Ficoll. Then, 0.5 times 106 to 1 times 106 cells were transferred intravenously into NOD Rag2-/- or NOD Tcra-/- mice. Blood glucose concentrations were measured with an Accu-Chek glucose meter (Roche).

Foxp3 methylation analysis.

Sort-purified cells were assessed by bisulphite sequence analysis21. Methylation-specific PCR primer sequences were 5'-TATTTTTTTGGGTTTTGGGATATTA-3' (forward) and 5'-AACCAACCAACTTCCTACACTATCTAT-3' (reverse).

TCR repertoire analysis.

YFP-GFP-, YFP+GFP- and YFP+GFP+ Valpha2 TCR clones (384 each) were sequenced by McLab. A Python script was used for extraction of full-length sequences, which were then trimmed to include only the PCR-amplified TCR Valpha2 domains. Sequences were submitted by batch to the International Immunogenetics Information System website for V-gene and joining-gene analysis. Of the original 384 clones per cell population, 227 Treg cells, 202 YFP+GFP- cells and 236 Tconv cells had productive V- and joining-gene rearrangements. A separate script was used for compilation of occurrences of each oligonucleotide and CDR3 peptide sequence in each cell population and for comparison of occurrences among the three populations.

Isolation of lymphocytes from pancreas.

Pancreases were excised independently of lymph nodes and were incubated for 30 min at 37 °C in collagenase P (1 mg/ml; Roche), DNase (20 mug/ml) and 0.2% (wt/vol) BSA in RPMI medium. Digested tissue was strained through a 70-muM cell strainer (BD Biosciences) and was washed once with RPMI medium containing DNase. Lymphocytes were separated from low-density pancreatic cells by centrifugation through a 40%–60% (vol/vol) percoll gradient. Lymphocytes were washed and stained for flow cytometry.